

# Characterising appearance of gold foils and gilding in conservation and restoration

Yoko Arteaga<sup>1,2,\*</sup>, Aditya Sole<sup>2</sup>, Jon Yngve Hardeberg<sup>2</sup> and Clotilde Boust<sup>1,3</sup>

<sup>1</sup>Centre for Research and Restoration of the Museums of France, Palais du Louvre, Porte des Lions, 14 quai François Mitterrand, 75001 Paris, France

<sup>2</sup>Colourlab, Norwegian University of Science and Technology, Teknologivegen 22, 2815 Gjøvik, Norway

<sup>3</sup>PSL-PCMTH UMR8247, CNRS, 11 Rue Pierre et Marie Curie, 75005 Paris, France

## Abstract

Materials with complex optical properties like gold foils are commonly used for gilding in the field of conservation and restoration to render the visual appearance of the restoration object. Characterising the appearance of these materials is important to render an accurate visual appearance that can be obtained with different gilding techniques. In this paper, the bidirectional reflectance of gold foils commonly used for gilding is characterised and as well as gilding mock-ups. The dataset of gold foils is publicly available.

## Keywords

BRDF measurement, gold, material appearance

## 1. Introduction

Gold material is commonly found in artworks in the form of gilding. In the past, artists used gold not only because of its cultural and religious importance but also because of its interesting appearance properties. Gilding is a form of polychromy found in medieval paintings and altarpieces [1]. It consists of a ground layer where a gold foil is attached to by different means. Different gilding techniques render different appearances. For example, oil gilding is known to have a matte and rough appearance whereas water gilding is smooth and glossy due to the final burnishing process using an agate stone [2].

In the field of conservation, it is important to have a deep understanding of the properties of different materials and how they contribute to the original appearance of surfaces. Gilding is a composite material in which its elements are arranged in layers, gold being one of them. It is thus, vital to characterise the appearance of the gold layer in the gilding to carry out better conservation campaigns which can render a more faithful appearance of the gilded object.

Gold material shows complex reflectance properties as its appearance changes with the change in the illumination direction [3]. Characterising the appearance of such materials is therefore difficult using the reflectance measurement geometries (like 0:diffuse, and 0:45) defined by the

---

*The 11<sup>th</sup> Colour and Visual Computing Symposium, September 08–09, 2022, Gjøvik, Norway*


\*Corresponding author.

✉ yoko.arteaga@culture.gouv.fr (Y. Arteaga); aditya.sole@ntnu.no (A. Sole); jon.hardeberg@ntnu.no (J. Y. Hardeberg); clotilde.boust@culture.gouv.fr (C. Boust)

🆔 0000-0002-6787-789X (Y. Arteaga); 0000-0002-7916-5363 (A. Sole); 0000-0003-1150-2498 (J. Y. Hardeberg); 0000-0001-6019-1118 (C. Boust)



© 2022 Copyright for this paper by its authors. Use permitted under Creative Commons License Attribution 4.0 International (CC BY 4.0).

 CEUR Workshop Proceedings (CEUR-WS.org)

standardising bodies like ASTM and ISO. Bidirectional reflectance measurements are therefore necessary to characterise these materials appearance. Bidirectional reflectance measurements are performed using multi-angle spectrophotometers and goniospectrophotometers. Moreover, various types of gold foils are used in gilding that vary in karat, composition, and provenance which affects the gilding appearance visually. Famous examples besides traditional gold are white gold and rose gold [1].

In this paper, ten different gold foils commonly used for restoration, and two gilding mock-ups made by professional restorers have been bidirectionally measured and characterised using a bidirectional reflectance measurement device and a well established reflectance model. The gilding mock-ups are produced using one of the gold foils presented in this paper.

The structure of the paper is as follows: the next section of this paper presents a brief literature review of appearance modelling of gold and gilding. The third section presents the gold foils used and describes the fabrication method of the gilding mock-ups, the setup used for the bidirectional measurements, and the reflectance model fitting. Finally, the results and discussion are presented followed by the conclusion and final remarks.

## **2. Background**

### **2.1. Appearance modelling of gold and gilding in restoration**

Several attempts have been made to model and render the appearance of gold surfaces in cultural heritage objects. Callet et al. [4] proposed an empirical model based on the metallic structure of gold and used Kubelka Munk's two flux theory to render the gilding of polychrome statues.

The influence of the colour of the substrate on the appearance of gilding is actively studied within the field of cultural heritage and has been tested empirically by Dumazet et al. [5] by changing the colour of the substrate in their model and thus rendering different appearances of gilded surface. A similar study has been carried out by Mounier et al. [6] on medieval mural paintings. Mounier et al. [6] observed that the final appearance of the gilding is affected by the substrate colour.

Wu et al. [7] studied the influence of the substrate colour on the gild appearance by fabricating gilding mock-ups using different methods such as oil gilding, water gilding and ground gilding. Colorimetric and interferometric microscopic measurements were made to characterise the mock-ups. They concluded that the colour of the substrate does not alter the visual appearance of gilding. However, it was observed that burnishing the gild shows a significant visual change in its appearance.

MacDonald et al. [8] conducted a round-robin test to evaluate the quality of different multi- and hyper-spectral imaging devices both in terms of spectral and spatial quality. They studied objects with metal like finish and golden appearance. It was observed that the specularly of the surface and the golden appearance of the object increase the difficulty of accurately reproducing both colour and spectral characteristics of the object.

In [9] an HDR hyperspectral imaging methodology was proposed to accurately capture the reflectance spectra of an illuminated image with gold areas. The diffuse reflectance was then rendered within an uniform dynamic range.

A different type of gilding is found in medieval sculptures in Norway where instead of using a gold foil, a silver foil is used and then a yellow resin is applied to it, which gives the appearance of gold. In [10], bidirectional reflectance measurements of these samples are performed. It was observed that the samples showed two specular peaks due to its composite structure. One being from the interface air-resin and one from the interface resin-silver.

## 2.2. Bidirectional reflectance modelling

Bidirectional reflectance of a material can be modelled using a distribution function called bidirectional reflectance distribution function (BRDF) defined by Nicodemus in [11]. A BRDF describes how light is reflected off a surface. It is defined by the ratio between the differential irradiance along  $\mathbf{l}$  at point  $x$  and the differential outgoing radiance along  $\mathbf{v}$ :

$$f(x, \mathbf{l}, \mathbf{v}) = \frac{dL_r(x, \mathbf{v})}{dE(x, \mathbf{l})} \quad (1)$$

For a BRDF model to be physically valid it must obey two properties: be energy conserving and reciprocal. Due to the law of conservation of energy, the radiant energy reflected at a surface must not be greater than the energy incident on the surface. The second property is known as Helmholtz reciprocity, which dictates that the BRDF must be symmetrical. This means that reversing incoming and outgoing light does not change the BRDF outcome.

BRDF of a material can be further divided into isotropic and anisotropic. Regular surfaces with a rotational symmetry are called isotropic and the BRDF is expressed as  $f(x, \theta_i, \theta_r)$ , following the notation in Figure 4. Anisotropic surfaces exhibit a change in BRDF when rotated around the surface normal, giving  $f(x, \theta_i, \phi_i, \theta_r, \phi_r)$ .

A number of empirical and physical reflectance models have been defined till now to model different types of materials and for applications [12]. Cook-Torrance (CT) is a well established physical model and is used extensively to model specular materials like gold [3, 13, 14].

### 2.2.1. Cook-Torrance BRDF:

Cook-Torrance (CT) is a physical model based on the micro-facet theory [13]. CT model consists of specular and diffuse reflection components and mathematically is defined as follows:

$$f = k_d R_d + k_s R_s, \quad (2)$$

In Eq. 2,  $k_d$  and  $k_s$  are weighting parameters and  $k_d + k_s = 1$ . The specular term is based on micro-facet theory, which dictates that only the micro-facets on the surface with orientations in between the viewing vector and the incident vector, called half-vector  $\mathbf{h} = \mathbf{l}, \mathbf{v}$ , will contribute to the reflected light.

The general form of the CT specular term is:

$$R_s = \frac{1}{\pi} \frac{FDG}{(\mathbf{n}, \mathbf{l})(\mathbf{n}, \mathbf{v})}, \quad (3)$$

where  $F$  is the Fresnel term [15],  $G$  is the geometrical attenuation factor accounting for shadowing and masking of micro-facets, and  $D$  is the distribution of normals facing  $\mathbf{h}$ .

**GGX distribution** Walter et al. [16] propose a Bidirectional Scattering Distribution Function (BSDF) called GGX. This GGX BRDF is inspired by the micro-facet model proposed by Cook and Torrance. The general form of the GGX is given by:

$$R_s = \frac{1}{4} \frac{FDG}{(\mathbf{n} \cdot \mathbf{l})(\mathbf{n} \cdot \mathbf{v})}, \quad (4)$$

which is the same as the general form of the Cook-Torrance in Eq. 3, except that the normalisation factor for the Fresnel term is changed to 4. The Fresnel term in the GGX distribution is the same as the one proposed by Cook and Torrance. The GGX normal distribution function of micro-facets is given by:

$$D = \frac{\alpha_g^2 \chi^+(\mathbf{h} \cdot \mathbf{n})}{\pi \cos^4 \theta_h (\alpha_g^2 + \tan^2 \alpha_h)^2}, \quad (5)$$

where  $\alpha_g$  is a width parameter for the specular lobe,  $\theta_h$  is the angle between the half-vector,  $\mathbf{h}$ , and the surface normal,  $\mathbf{n}$ , and  $\chi^+$  is a positive characteristic function which equals to one if its parameter is greater than zero and zero if its parameter is lesser or equal to zero.

The geometrical attenuation factor which describes the shadowing and masking effects in the GGX is derived from D. This is given by the monodirectional shadowing term defined as

$$G_1(\mathbf{v}) = \chi^+ \left( \frac{\mathbf{v} \cdot \mathbf{h}}{\mathbf{v} \cdot \mathbf{n}} \right) \frac{2}{1 + \sqrt{1 + \alpha_g^2 \tan^2 \theta_v}}, \quad (6)$$

where  $\theta_v$  is the angle between the viewing vector  $\mathbf{v}$  and the surface normal  $\mathbf{n}$ .

### 2.3. BRDF metrics

When optimising a BRDF model, different metrics can be used to find the best approximation to the surface reflectance. There is no consensus in the literature as to which metric should be used. A common metric to use is the Root Mean Square error (RMSE). In [17], the BRDF of a set of materials is estimated using different error metrics. The estimated BRDFs are then tested in a psychophysical experiment to correlate the choice of error metric and perceived appearance. The authors find that while metrics such as RMSE can provide a good optimisation when evaluating the BRDF plot, this does not always correlate to a faithful appearance reproduction if the rendered images are compared.

## 3. Method

### 3.1. Measurement samples: Gold foils

Ten gold foils that are commonly used in restoration were measured bidirectionally using a multiangle spectrophotometer. Table 1 gives the name and specification of these 10 gold foils. Since an extremely thin layer (approximately 0.2 microns in thickness) of the gold foils is used for gilding, the foil samples were prepared by a professional restorer to allow for production

**Table 1**

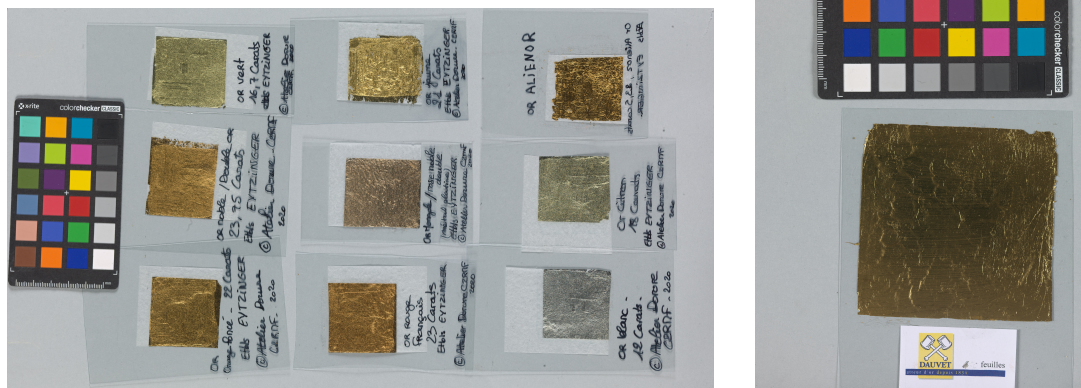
Specifications of the gold foils used. ©C2RMF/Stéphanie Courtier.

Name	Colour	Karat	Manufacturer
Or Alienor	Deep yellow/orange	23.5	Dauvet (FR)
Or Blanc	Light grey	12	Eytzinger (DE)
Or Citron	Light yellow	18	Eytzinger (DE)
Or Jaune	Deep yellow	21	Eytzinger (DE)
Or Noble	Deep yellow/orange	23.75	Eytzinger (DE)
Or Orange	Deep orange	22	Eytzinger (DE)
Or Rose	Rose	22	Eytzinger (DE)
Or Rouge	Deep orange/red	23	Eytzinger (DE)
Or Versailles	Deep yellow	22	Dauvet (FR)
Or Vert	Light yellow/green	16.7	Eytzinger (DE)

accuracy, layer uniformity, sample transportation, and measurement possibility. The gold foils have been prepared following the steps of oil gilding as follows:

- A ground layer of glue is applied to an acrylic sheet,
- When the glue is sticky, the gold foil is placed on top of the glue with the aid of a trowel and a gilder's tip, illustrated in Figure 2a,
- A gilder's duster is used to tap on any air bubbles which may have formed between the gold sheet and the acrylic.

Figure 1 shows the 10 gold foils used in this study.



(a) or Orange, or Noble, or Vert, or Rouge, or Rose, or Jaune, or Blanc, or (b) or Versailles used for the gilding mock-ups

**Figure 1:** Gold foil samples

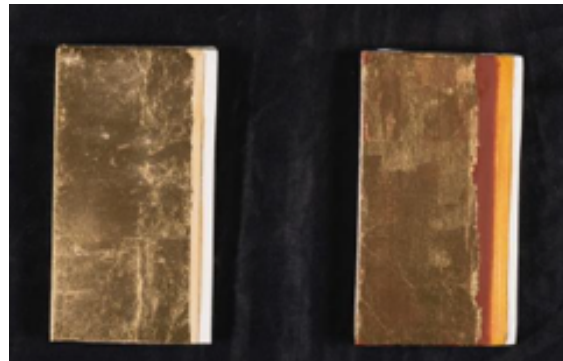
### 3.1.1. Gilding samples:

Gilding using the gold foils can be carried out using 2 well established techniques called water gilding, and oil gilding. In both the techniques, a wood piece surface is first prepared using a ground layer made of chalk diluted with rabbit skin glue. In the water gilding technique, a substrate layer of red coloured clay, called bole, is applied to the surface and is made wet using ethanol and water before the gold foil is applied to it. In the next step, excess water (if any) is removed using a gilder's duster. The gold foil is then burnished manually with an agate stone in a single direction of the surface plane. This process gives the surface a very high gloss. The water gilding technique is therefore also known as "glossy gilding" technique.

In the oil gilding technique, a layer of oil-based adhesive called 'gold-size' is used as both, the substrate and adhesive. When the gold-size is tacky but not completely dry, the gold foil is applied to it using a gilder's tip. Due to the nature of the gold size it is not possible to burnish this surface, giving it a matte finish.



(a) Gold foil on a gilders cushion, cut with a trowel before being placed on the substrate using the gilder's tip (pink)  
©C2RMF/Stéphanie Courtier



(b) Gilding mock-ups.  
Oil gilding on the left and water gilding on the right. ©Inp/Angèle Dequier

### 3.2. Bidirectional reflectance measurements

Bidirectional reflectance from the gold foil sample surface was measured using an X-Rite MA-T12 multi-angle spectrophotometer. The MA-T12 instrument measures at six illumination sources and two pick-up points according to the specifications of industry standards for metallic colours [18, 19, 20]. It measures surface reflectance in the ranges of 400 - 700nm at 10nm

intervals. The illumination source is a polychromatic white LED with blue enhancement and its spot size is of 9 mm by 12 mm. Figure 3 illustrates the combination of illumination and viewing directions obtained by the MA-T12.

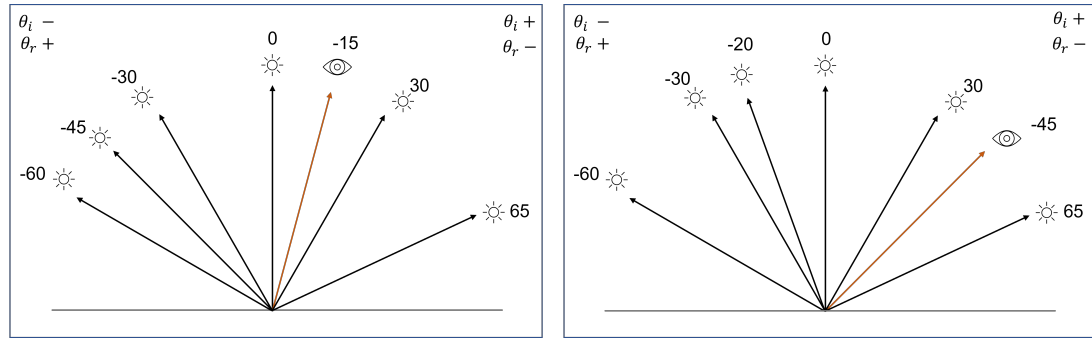


**Figure 3:** Measurement geometry of the MA-T12. **Left:** Illumination directions for viewing at  $-15^\circ$ . **Right:** Illumination directions for viewing at  $-45^\circ$ .

For each gold foil the measurements were repeated at five different locations, illustrated in Figure 4. For each location, the MA-T12 was rotated clockwise around the normal, four times. Since each measurement of the MA-T12 gives 12 spectra, 48 reflectance spectra were measured per area at five different locations, giving a total of 240 reflectance spectra per sample. Table 2 shows all the combinations of incidence and viewing directions. The convention for the angles is illustrated in Figure 4. The elevation angle ( $\theta$ ) ranges from  $-90^\circ$  to  $90^\circ$  and is measured from the normal of the surface and the azimuth angle ( $\phi$ ) ranges from  $0^\circ$  to  $360^\circ$  and is measured clockwise from the x-axis. Illumination directions are positive clockwise from the normal and viewing directions are positive anti-clockwise from the normal.

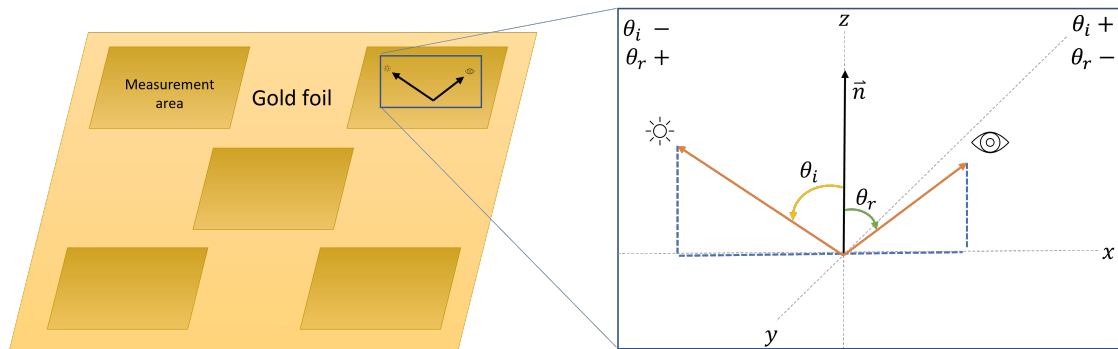


**Figure 4:** **Left:** Diagram representing five areas measured for each gold foil: the four corners and the centre. **Right:** Proposed parametrisation of the BRDF as a function of ( $\theta_i$ ) and ( $\theta_r$ ). For each area in the gold foil 48 reflectance spectra are taken.

The gilding mock-ups were measured in the same way as the gold foils with the exception that the measurement was not repeated at different areas due to limited sample surface size.

**Table 2**

Elevation and azimuth angles for incident and viewing positions. The elevation angles are given from the normal of the surface and the azimuth angles are given clockwise from the x-axis. All angles are in degrees.

Illumination direction ( $\theta_i$ )	Viewing direction ( $\theta_r$ )
-15°	-60° -45° -30° 0° 30° 65°
-45°	-60° -30° -20° 0° 30° 65°
Illumination azimuth ( $\phi_i$ )	Viewing azimuth ( $\phi_r$ )
0° 90° 180° 270°	180° 270° 0° 90°

### 3.3. BRDF fitting

Spectral reflectance measurements obtained from the MA-T12 were used to train the isotropic CT model with the GGX distribution. The model was trained in the CIEXYZ colorimetric space. CIEXYZ values were calculated using Equation (7). In Equation (7),  $r(\lambda)$  is the measured spectral reflectance at the sample surface,  $S(\lambda)$  is the spectral power distribution of the D65 illuminant, and  $\bar{x}(\lambda)$ ,  $\bar{y}(\lambda)$ ,  $\bar{z}(\lambda)$  are the CIE 1964 colour matching functions,

$$\begin{bmatrix} X \\ Y \\ Z \end{bmatrix} = \frac{1}{N} \int_{\lambda} S(\lambda) r(\lambda) \begin{bmatrix} \bar{x}(\lambda) \\ \bar{y}(\lambda) \\ \bar{z}(\lambda) \end{bmatrix} d\lambda, \quad (7)$$

where

$$N = \int_{\lambda} r(\lambda) \bar{y}(\lambda) d\lambda. \quad (8)$$

The diffuse reflection component coefficient ( $R_d$ ) in the CT model was optimised individually ( $R_{dX}$ ,  $R_{dY}$ , and  $R_{dZ}$ ) in the CIEXYZ colour space while a single coefficient for the specular reflection ( $R_s$ ) and roughness ( $m$ ) component was optimised across CIEXYZ as shown in Equation (9).

$$I_P = s \begin{bmatrix} I_{Px} \\ I_{Py} \\ I_{Pz} \end{bmatrix} = I_a R_a + I_i \cos \theta_i \left( k_s R_s + (1 - k_s) \begin{bmatrix} R_{dX} \\ R_{dY} \\ R_{dZ} \end{bmatrix} \right) \quad (9)$$

In Equation (9),  $I_P$  is the CIE tristimulus value at point P with illumination direction  $\theta_i$  and viewing direction  $\theta_r$ .  $I_a R_a$  is the ambient light term which is assumed to be zero as the experiment is performed in a dark environment.  $I_i$  is the incident light intensity,  $R_{dXYZ}$  are the diffuse reflectance components to be optimised. The specular components  $R_s$  are given by Equation 4 following the GGX distribution of micro-facets normals.

An extra parameter  $s$  is optimised as a scaling factor due to the fact the CIE Y values go well above one. This is because the domain is limited to that of a white Lambertian surface and in this case the samples have reflectance values above one. The scaling parameter violates the conservation of energy constraint of the BRDF model but it is necessary to add it in order to fit the model. To simplify the optimisation problem, the diffuse component  $R_d$  is not estimated



and the value at 0/45 measurement geometry is used. Using a genetic algorithm, the RMSE formula is used as an objective function and only the CIE Y value is estimated. The RMSE is given by

$$RMSE = \sqrt{\frac{\sum((M(\theta_i, \theta_r) - E(\theta_i, \theta_r, p))^2)}{n}}, \quad (10)$$

where  $M$  are the measured CIE XYZ values (Eq. 7) and  $E$  are the estimated BRDF values obtained using the Cook-Torrance GGX BRDF model (Eq. 9), with the parameters  $p$ , calculated for the  $n$  pairs of incident and reflected directions.

## 4. Results and Discussion

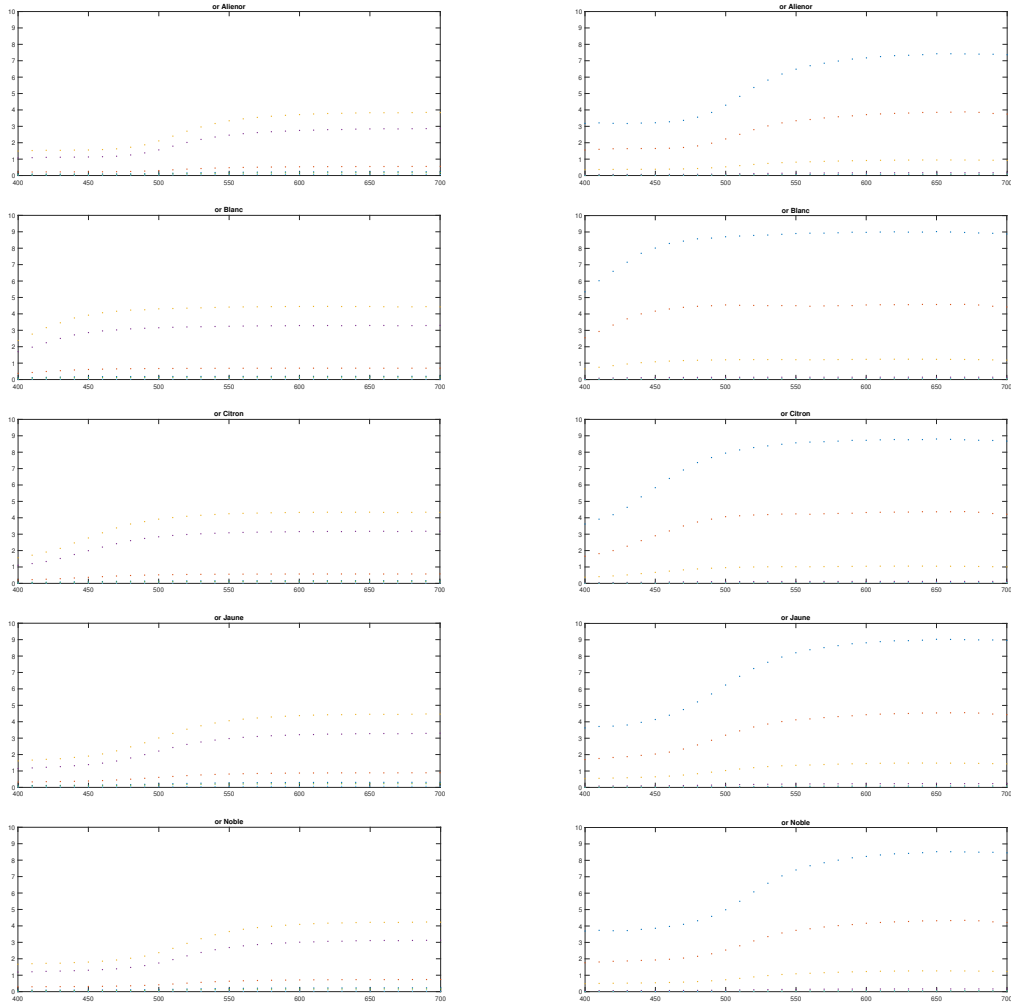
The gold foils and gilding mock-ups were measured to obtain their bi-directional reflectance according to the geometries previously described. CIE L\*a\*b\* values are calculated and to evaluate the luminance of the samples, the L\* values are analysed as a function of angle of incidence. A BRDF model is estimated for the gilding mock-ups and the gold foil used for their fabrication, namely Or Versailles.

All the gold foils have a different appearance due to their karat composition, which gives them a different colour. However, due to the metallic properties of gold and the fact that the gold foils have been produced in a similar way, they should have a similar shine. On the contrary, the gilding mock-ups have been manufactured using techniques which alter the surface of the gold foil and thus, the shape of their BRDF is expected to be different even if their diffuse colour is similar to that of the original gold leaf.

### 4.1. Gold foils: colour and reflectance spectra

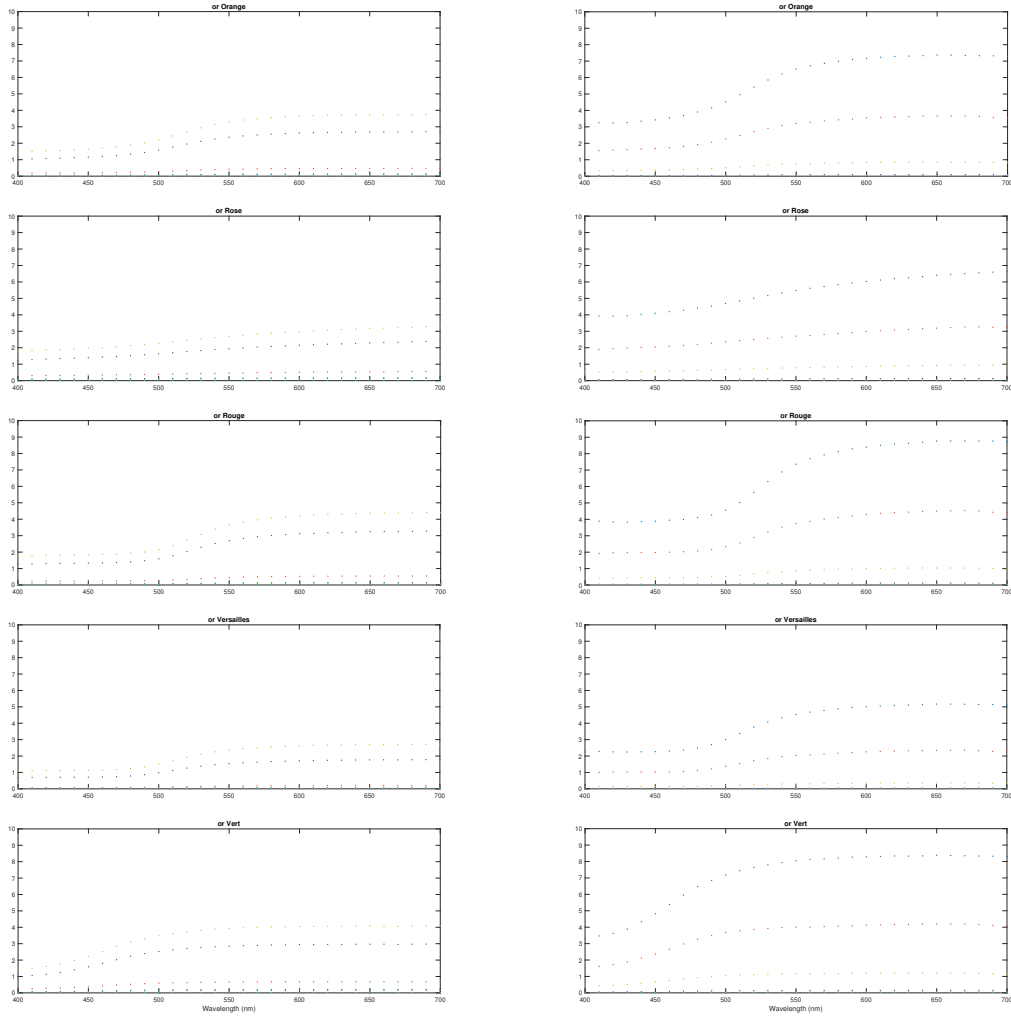
The reflectance spectra of the gold foils is plotted as a function of wavelength in the visible spectrum range from 400 to 700 nm in Figure 5 and Figure 6. The measurement geometries are specified in Table 2. All the measurements have been averaged, regardless of their location in the gold foil and the orientation of measurement, assuming the samples are isotropic. The curves are smooth and for all samples at both viewing angles the reflectance factors go above one at illumination directions  $-30^\circ$  and  $0^\circ$  (yellow and purple curves), and  $-60^\circ$  and  $-45^\circ$  (blue and orange curves) respectively. This is because the white reference used is a Lambertian white reference which assumes a value of one for all directions and wavelengths. The different gold foils reflectance curves have more or less contribution on the longer end of the spectrum depending on their colour.

Figure 7, shows the sRGB visualisation of the gold foils at all measurement geometries. The rendering was done using CIE standard observer  $10^\circ$  colour matching functions and D65 illuminant. As described previously, each gold foil has a different hue due to its different karat composition. The colour is rendered as white in the case of all gold foils except Or Versailles at angles of incidence  $-30^\circ$  and  $0^\circ$  for viewing direction  $-15^\circ$ , and  $-60^\circ$  and  $-30^\circ$  for viewing direction  $-45^\circ$ . This is because the reflectance factors exceed one for these measurement geometries and thus the luminance of the samples cannot be rendered in a standard dynamic range display.



**Figure 5:** Reflectance curve of gold foils (1/2). The viewing angles are  $-15^\circ$  and  $-45^\circ$ . For each viewing direction the illumination directions are defined in Table 2.

Figure 8 shows the mean CIE  $L^*$  value for all gold foils as a function of the illumination direction. The error bars represent two standard deviations. For all gold foils the value of  $L^*$  greatly increases as the illumination angle approaches the mirror angle. The values of  $L^*$  go much higher than 100 because the spectrophotometer is taking the reference white to be a Lambertian white surface.



**Figure 6:** Reflectance curve of gold foils (2/2). The viewing angles are  $-15^\circ$  and  $-45^\circ$ . For each viewing direction the illumination directions are defined in Table 2.

## 4.2. Gold foils: bidirectional measurements

### 4.3. Comparing gold foil, water gilding, and oil gilding

Different manual processes and techniques are expected to alter the surface of the gold foil and change its appearance when used for gilding. While oil gilding is known to have a more matte appearance, water gilding has a higher gloss due to the final burnishing step which is not performed in the former.

Figure 9, shows the CIE Y values as a function of the illumination direction for the oil gilding mock-up, water gilding mock-up and Or Versailles gold foil at viewing directions  $-15^\circ$  and  $-45^\circ$ . These samples have also been used to train a BRDF model using the GGX distribution and a genetic algorithm to optimise the RMSE as objective function. The BRDF model was trained for

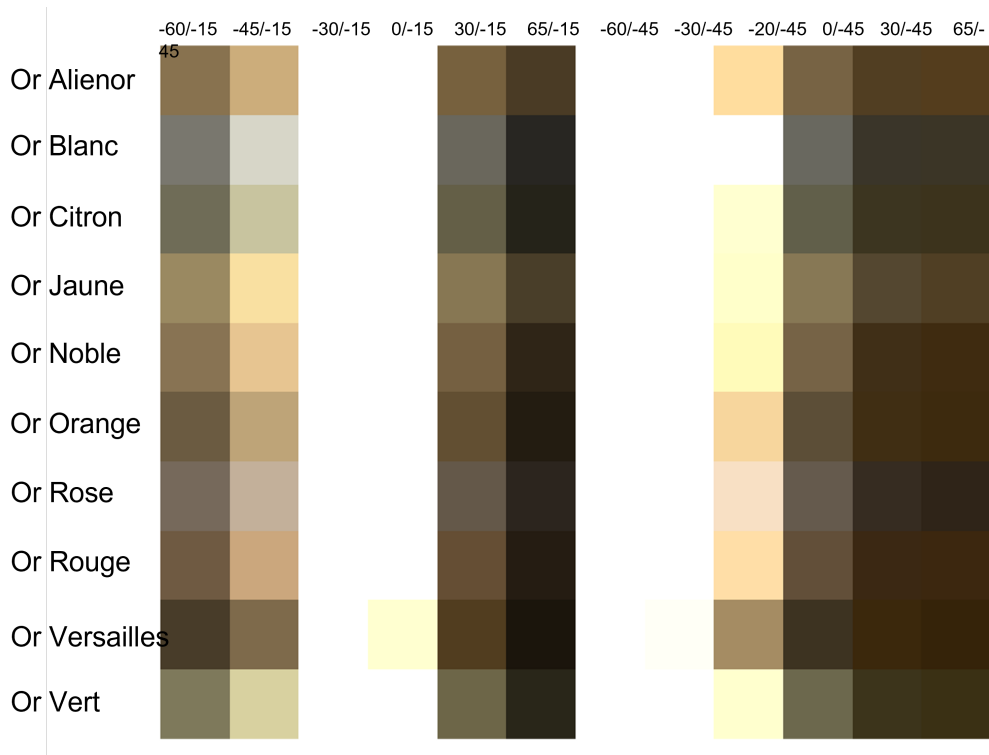


**Figure 7:** sRGB visualisation of the gold foils at all measurement geometries using CIE standard observer 10° colour matching functions and illuminant D65.

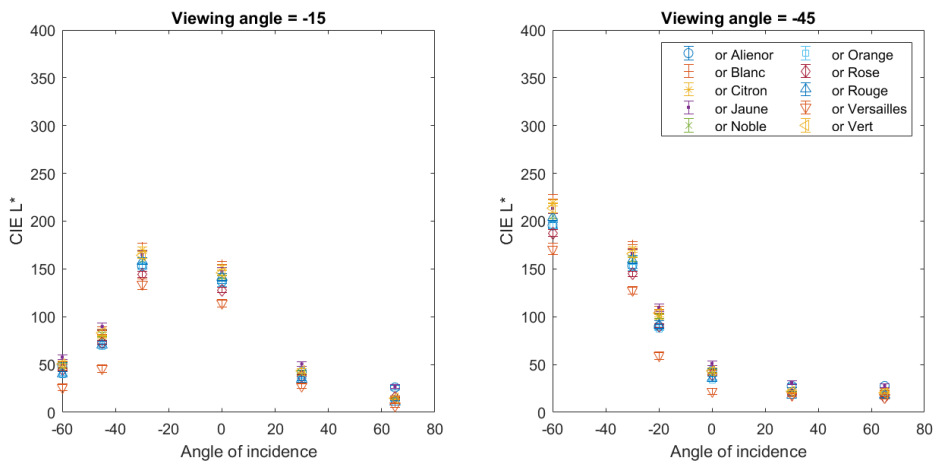


**Figure 8:** Measured CIE  $L^*$  of gold foils at viewing directions  $-15^\circ$  (left) and  $-45^\circ$  (right).

each viewing direction rather than training a single model with both viewing directions. This is because the data is sparsely sampled and an acceptable model that satisfied both viewing directions was not achieved.

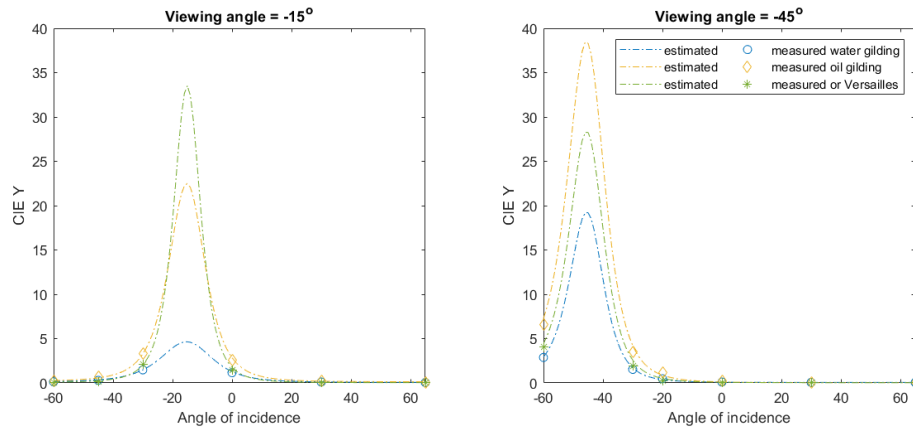


**Figure 9:** Measured CIE Y at viewing angle  $-15^\circ$  (left) and  $-45^\circ$  (right) respectively. BRDF model with estimated parameters in Table 3

**Table 3**

BRDF model estimated parameters using GGX distribution and genetic algorithm to optimise RMSE.

	Water gilding		Oil gilding		Or Versailles	
	$-15^\circ$	$-45^\circ$	$-15^\circ$	$-45^\circ$	$-15^\circ$	$-45^\circ$
Scaling factor	1.506	2.086	3.092	3.379	2.951	3.156
$k_s$	0.694	0.667	0.819	0.988	0.706	0.672
$\alpha$	0.137	0.090	0.096	0.099	0.071	0.092

The BRDF parameters estimated and used to plot the values in Figure 9 are shown in Table 3. The scaling factor was limited to the range  $[0, 5]$  and both  $k_s$  and  $\alpha$  defined in the range  $[0, 1]$ .

The three samples show a similar behaviour at both viewing directions. At viewing direction  $-15^\circ$ , oil gilding shows the highest values of CIE Y for all angles of illumination. The gold foil has lower values of CIE Y for angles further from the mirror angle, but for angles of illumination  $-30^\circ$  and  $0^\circ$ , the water gilding has the lowest values of CIE Y. The same trend is seen at viewing direction  $-45^\circ$ . However, the BRDF models show a different relative difference between the samples. At viewing direction  $-15^\circ$ , water gilding has a much lower peak than oil gilding and the gold foil has the highest peak. On the other hand, for  $-45^\circ$  viewing direction, oil gilding has the highest peak. The shape of the curves is more similar at this viewing direction as well.

The gloss of the water gilding and oil gilding mock-ups was measured using a Rhopoint IQ glossmeter. Table 4 shows the gloss values obtained at  $20^\circ$ ,  $60^\circ$  and  $85^\circ$  geometry. It can be seen that water gilding has a much higher gloss than oil gilding.

#### 4.4. Discussion and future work

Complex materials such as gold foils and gilding present particular appearance properties which cannot be simply described by colorimetry. Moreover, the metallic nature of the samples requires the specular peak to be sampled with a fine resolution to properly characterise these

**Table 4**

Gloss measurements of water and oil gilding. The measurements were done using a Rhopoint IQ glossmeter.

	Gloss 20	Gloss 60	Gloss 85
Water gilding	315	360	77
Oil gilding	25	85	22

surfaces.

In the field of heritage science, gilded or golden surfaces are frequently characterised by colour measurements performed at single measurement geometries. Normally, measurements are done in a diffuse domain for example 0/45, which is insufficient to properly describe the appearance of gold. In Figure 7, the sRGB render of the reflectances at different measurement geometries shows that the colour of gold is very different from the visual perception that observers have of these materials. For example at 0/-45, column ten in Figure 7, the colour of the gold foils is very dark.

Evidently, pure colour measurements are not sufficient to properly characterise the appearance of golden surfaces. As demonstrated, a BRDF model certainly can help to render the appearance of gold and gilding in more realistic way which is related to visual perception. An attempt to estimate the BRDF model of the gilding mock ups and its gold foil was presented in Figure 9.

The BRDF models obtained fail to properly characterise the differences in appearance of the gold foil, water gilding, and oil gilding. This is probably due to the fact the BRDF model is a data hungry model which requires more number of measurements to train coefficients that can accurately represent the surface at many combinations of angles of incidence and viewing. In this paper, the models are trained with six measurements for each viewing direction and moreover, the reflectances are not sampled at angles close to the specular peak. The fact that the BRDF model is trained on each individual viewing direction independently rather than just having a single model does not allow for the models to then be directly comparable. This is because the specular peak is unknown and thus the model cannot be properly trained.

Finally, a remark must be made on the fact that the gilding mock-ups have been made with the same gold foil. The only difference between the pure gold foil (Or Versailles), the oil gilding mock-up, and the water gilding mock-up is the orientation of the micro-facets of each surface. The Fresnel coefficient of the three surfaces will be the same since the chemical composition of the gold foil is unchanged by either gilding techniques. The amount of radiance being absorbed by the three surfaces is the same. Thus, the distribution of the scattered rays can be normalised over all incident directions to a constant that will be the same for the three surfaces.

Future work should include improvement in the fitting of the BRDF model. Although the Cook-Torrance BRDF model using a GGX distribution seems to be the appropriate model for the samples, some limitations have to be overcome to obtain more faithful models. First of all, the high specularity of the surfaces must be accounted in the BRDF model so the scaling factor is not violating any rule such as conservation of energy. Additionally, the lack of data close to the specular peak requires that some assumptions are to be made to characterise these. For example, the fact that the Fresnel coefficient of the surfaces is the same should be exploited.

Moreover, once the BRDF models are obtained, they will have to be evaluated. It would be valuable to perform a psychophysical experiment to evaluate how good the models are at rendering the subtleties in appearance difference between these surfaces. Also, the models can be tested for their ability to characterise the surfaces with respect to each other by performing a classification task based on the coefficients.

In the field of conservation science, it would be valuable to understand how the different gilding techniques change the BRDF model and thus the appearance of the surfaces. This could give insights into restoration techniques and procedures that render an appearance closest to that of the original gilding. Another interesting possibility would be to characterise the effects of ageing on gilded surfaces in order to create a model linking the original appearance of the gilding and its aged appearance for virtual restoration purposes.

## 5. Conclusion

In this paper, ten different gold foils commonly used for restoration have been measured and characterised using a bidirectional reflectance measurement device and an well established reflectance model. Two types of gilding mock-ups, water gilding and oil gilding, fabricated with one of the gold foils studied, have also been measured. It is found that the gold foils and gilded mock-ups are very specular and present reflectance factors higher than one at angles as close as 15° from the mirror angle.

It is found that these measurement angles are not enough to fit a BRDF model that accurately describes the appearance of the surfaces. It is suggested that the model is modified so the high specularity of the surface is better described. Also, given the surfaces should have the same transmittance and absorption, the BRDF models can be normalised to have the same value over all angles of incidence.

## Acknowledgments

This work has received funding from the European Union's Horizon 2020 research and innovation program under grant agreement No. 813789, through the the MSCA ITN project CHANGE (<https://change-itn.eu/>).

We would like to thank Stéphanie Courtier from the Centre of Research and Restoration of the Museums of France, for her help in the preparation of samples.

## References

- [1] K. Kollandsrud, U. Plahter, Twelfth and early thirteenth century polychromy at the northernmost edge of europe: past analyses and future research, *Medievalista online* (2019). URL: <https://dx.doi.org/10.4000/medievalista.2303>. doi:10.4000/medievalista.2303.
- [2] G. P. Mastrotheodoros, K. G. Beltsios, Y. Bassiakos, V. Papadopoulou, On the metal-leaf decorations of post-byzantine greek icons, *Archaeometry* 60 (2018) 269–289. URL: <https://onlinelibrary.wiley.com/doi/abs/10.1111/arcm.12287>. doi:<https://doi.org/10.1111/arcm.12287>.

- [3] A. Sole, G. C. Guarnera, I. Farup, P. Nussbaum, Measurement and rendering of complex non-diffuse and goniochromatic packaging materials, *The Visual Computer* 37 (2021) 2207–2220.
- [4] P. Callet, A. Zymła, A. Mofakhami, Virtual metallurgy and archaeology. application to the visual simulation of a work of art, in: ICCVG, 2002, pp. 25–29.
- [5] S. Dumazet, A. Genty, A. Zymła, F. De Contencin, A. Texier, N. Ruscassier, B. Bonnet, P. Callet, Influence of the substrate colour on the visual appearance of gilded sculptures, in: XXI International CIPA Symposium, 2007, pp. 01–06.
- [6] A. Mounier, F. Daniel, The role of the under-layer in the coloured perception of gildings in mediaeval mural paintings, *Open Journal of Archaeometry* 1 (2013). doi:10.4081/arc.2013.e16.
- [7] Q. Wu, M. Hauldenschild, B. Rösner, T. Lombardo, K. Schmidt-Ott, B. Watts, F. Nolting, D. Ganz, Does substrate colour affect the visual appearance of gilded medieval sculptures? part I: colorimetry and interferometric microscopy of gilded models, *Heritage Science* 8 (2020). doi:10.1186/s40494-020-00463-3.
- [8] L. W. MacDonald, T. Vitorino, M. Picollo, R. Pillay, M. Obarzanowski, J. Sobczyk, S. Nascimento, J. Linhares, Assessment of multispectral and hyperspectral imaging systems for digitisation of a Russian icon, *Heritage Science* 5 (2017). doi:10.1186/s40494-017-0154-1.
- [9] M. A. Martinez, E. M. Valero, J. L. Nieves, R. Blanc, E. Manzano, J. L. Vilchez, Multifocus hdr vis/nir hyperspectral imaging and its application to works of art, *Opt Express* 27 (2019) 11323–11338. doi:10.1364/OE.27.011323.
- [10] O. Sidorov, J. Y. Hardeberg, S. George, J. S. Harvey, H. E. Smithson, Changes in the visual appearance of polychrome wood caused by (accelerated) aging, in: *Electronic Imaging, Society for Imaging Science and Technology*, 2020, pp. 060–1–060–7. doi:doi.org/10.2352/ISSN.2470-1173.2020.5.MAAP-060.
- [11] F. E. Nicodemus, R. JC, et al., Geometrical considerations and nomenclature for reflectance. (1977).
- [12] D. Guarnera, G. C. Guarnera, A. Ghosh, C. Denk, M. Glencross, Brdf representation and acquisition, in: *Computer Graphics Forum*, volume 35, 2016, pp. 625–650.
- [13] R. L. Cook, K. E. Torrance, A reflectance model for computer graphics, *ACM Transactions on Graphics* 1 (1982) 7–24.
- [14] A. Sole, I. Farup, P. Nussbaum, S. Tominaga, Bidirectional reflectance measurement and reflection model fitting of complex materials using an image-based measurement setup, *Journal of Imaging* 4 (2018). URL: <https://www.mdpi.com/2313-433X/4/11/136>. doi:10.3390/jimaging4110136.
- [15] K. E. Torrance, E. M. Sparrow, Theory for off-specular reflection from roughened surfaces, *Journal of the Optical Society of America* 57 (1967) 1105–1112.
- [16] B. Walter, S. R. Marschner, H. Li, K. E. Torrance, Microfacet models for refraction through rough surfaces, in: *Eurographics conference on Rendering Techniques*, Eurographics Association, 2007, pp. 195–206.
- [17] A. Fores, J. Ferwerda, J. Gu, Toward a perceptually based metric for brdf modeling, in: *Color and imaging conference*, Society for Imaging Science and Technology, 2012, pp. 142–148.
- [18] *Standard Practice for Specifying the Geometry of Multiangle Spectrophotometers*, ASTM



- E2175-01, Standard, American Society for Testing and Materials, Pennsylvania, USA, 2001.
- [19] *Standard Practice for Multiangle Color Measurement of Metal Flake Pigmented Materials*, ASTM E2194-12, Standard, American Society for Testing and Materials, Pennsylvania, USA, 2012.
- [20] *Tolerances for Automotive Paint—Part 2: Goniochromatic Paints*, DIN 6175-2, Standard, Deutsches Institut für Normung, e.V, Berlin, DE, 2001.

## 6. Online Resources

The dataset of gold foils reflectances is available in the CHANGE-ITN repository (<https://zenodo.org/communities/change/?page=1&size=20>).